საქართველოს მეცნიერებათა ეროვნული აკადემიის მოამბე, ტ. 15, №2, 2021
BULLETIN OF THE GEORGIAN NATIONAL ACADEMY OF SCIENCES, vol. 15, no. 2, 2021

Physics

Growth of ZnO Microcrystals from Zn and Cu Chloride Precursors

Alexander Jishiashvili*, Zeinab Shiolashvili*, David Jishiashvili*, Archil Chirakadze*, Nino Makhatadze*

**V. Chavchanidze Institute of Cybernetics, Georgian Technical University, Tbilisi, Georgia*

(Presented by Academy Member George Japaridze)

The study of the growth mechanism of ZnO microcrystals at relatively low (~300°C) temperatures using $ZnCl_2$ and CuCl vapor showed that at 230°C the powdery layer of zinc and copper chloride particles was formed on Si substrate. In the local places of a layer the CuCl vapor produced the eutectic compositions with $ZnCl_2$, which have a low melting point of 241°C. As the substrate temperature exceeded that value, the eutectic compositions melted forming liquid droplets. The molten droplets were actively absorbing the ZnO vapor. Their oversaturation resulted in the precipitation of solid ZnO nuclei. The further growth of ZnO microcrystals proceeded through the Vapor-Solid mechanism forming rod-like crystals at 290°C, or elongated, one-dimensional ZnO structures at 330°C. *© 2021 Bull. Georg. Natl. Acad. Sci.*

ZnO microcrystal, vapor growth, zinc chloride, cuprous chloride

In the last decades the zinc oxide is intensively studied due to its unique properties. The wide and direct band gap (3.5 eV at 300K), lasing ability, piezoelectric properties, high stability of bi- and single excitons, good biocompatibility, high activity in photocatalysis and sensors are just a few examples of its outstanding features [1,2]. ZnO micro-and nanocrystals may be produced by a wide range of technologies. The choice of low-temperature growth methods is preferential for minimizing the thermal shocks on the substrate and components formed before ZnO growth, and for increasing the cost-effectiveness of the technology.

ZnO has a high melting (1975°C) and crystallization temperatures. However, the hydrothermal and wet-chemical technologies enable the synthesis of ZnO even at room temperature [3]. The vapor phase growth of ZnO, which is more versatile, clean, and "dry" technology, normally needs higher temperatures in the range of 500-1500°C [4]. Besides, thermodynamic restrictions hamper the nucleation of ZnO vapor on solid surfaces and it is common practice to form the initial ZnO seeds on a substrate [5].

The purpose of this work was to present the results of our study on the vapor growth of ZnO microcrystals at temperatures close to 300°C using CuCl and $ZnCl_2$ precursors.

Experimental

Microcrystals were produced in a vertical quartz reactor evacuated to 2×10^{-5} Torr. Its bottom, which was loaded with a mixture of ZnO (0.9 g), CuO (0.4 mg) and NH_4Cl (0.8 g) powders, was heated by an external furnace. Si substrate was placed on a vertical tubular quartz spacer just above the source and was heated by convection. Depending on the spacer height, the substrate temperature was 50-250°C lower than the source temperature. The growth process lasted 2 hour and included two stages. In the first stage, the temperature of the source and sample was gradually rising during the initial 15-20 minutes and then stabilized, reaching the pre-defined values. The second stage proceeded at a stabilized temperature. The substrate temperatures of 230, 290, 330°C were selected in the second stage of the growth. The corresponding source temperatures are indicated below.

Ammonium chloride decomposes at 195°C producing gaseous ammonia and HCl, which react with ZnO and CuO source powders forming $ZnCl_2$ and CuCl vapor. The former evaporates above 270°C [6], and the latter vaporizes as mono- and trimmers (Cu_3Cl_3) beginning from 447°C [7]. The saturated vapor pressures of these compounds are also different. At 265°C the pressure of $ZnCl_2$ ($P=7.5\times10^{-4}$ Torr [7]) is higher than that of CuCl ($P=1.2\times10^{-4}$ Torr [8]). However, at elevated temperatures P(CuCl) increases more abruptly than $P(ZnCl_2)$.

Results and Discussion

Fig. 1 (a) shows the Scanning Electron Microscopy (SEM) image of a product deposited on Si substrate heated up to 230°C. The source temperature was 450°C. The powdery layer of microparticles with average sizes of 2 micrometers was formed. Most of the particles were sintered producing flattened flakes. The composition of this layer was analyzed by Energy Dispersive Spectroscopy (EDS), which revealed the presence of Zn, Cl, Cu, and oxygen in the deposited layer. The Cu particles (Fig. 1, b) appeared because of the well-known reaction between Si substrate and CuCl: $4CuCl + Si = 4Cu + SiCl_4$ [9]. This is a spontaneous reaction with a high negative value of the Gibbs free energy difference in a wide range of temperature. As a result, the metallic Cu is formed, together with the volatile silicon tetrachloride, which boils at 57.7°C and readily evaporates at higher temperatures.

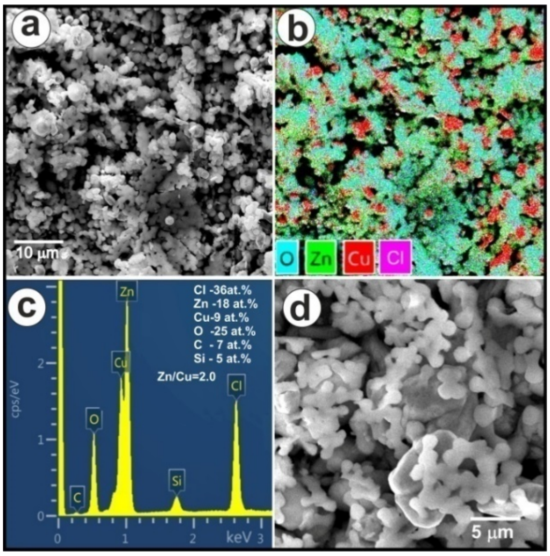

Fig. 1. SEM images of the layer produced on Si at 230°C and corresponding element map (a,b); EDS spectrum (c) and the enlarged surface element of the layer (d).

The additional information on the composition was obtained from FTIR spectrum (not presented in Fig. 1). Unfortunately, IR active vibrations of Cu-Cl bond lay between 368-222 cm^{-1}, which is below the detectable frequency of our IR device. As for $ZnCl_2$, it has an intense peak at 503 cm^{-1}, which corresponds to the stretching vibration of Zn-Cl bond [10]. We eliminated CuO from the source powder and used the mixture of ZnO and NH_4Cl as a source. The layer was grown on Si substrate at the same process parameters used for the synthesis of a material depicted in Fig. 1 (a). The IR spectrum of this layer confirmed the formation of $ZnCl_2$. Besides, the water molecule-related O-H stretching and H-O-H bending peaks were found at ~3400 and ~1600 cm^{-1}. These peaks appear because of the highly hygroscopic nature of $ZnCl_2$ that caused water uptake during the FTIR sample preparation. We assume that the major part of the oxygen signal in EDS spectrum was caused by the absorbed water. The pyrolytic formation of CuCl particles from $CuO+NH_4Cl$ source was also confirmed in our previous work [11].

The obtained results suggest that the layer depicted in Fig. 1 comprises CuCl and $ZnCl_2$ material. These compounds have limited solubility due to the differences in Cu and Zn valence, crystal structure of chlorides, and molecular configuration (linear in the case of $ZnCl_2$ and tetrahedral in CuCl) [6]. It should be emphasized that the growth temperature of the layer was below the melting points of both chlorides (CuCl = 423°C and $ZnCl_2$ = 290°C).

The SEM images of layers produced onto the substrate at 290°C are presented in Fig. 2 (a, b). Fig. 2 (c) shows the cathodoluminescence image of a surface depicted in Fig. 2 (b). The hexagonal rod-like microcrystals are sparsely nucleated on the substrate. The luminescence of hexagonal microcrystals suggests that they may have a direct band gap. The reliable information on their structure was obtained by Transmission Electron Microscopy (TEM) analysis. Fig. 2 (f) represents the TEM image and Selected Area Electron Diffraction (SAED) pattern of a thin microcrystal, which was placed onto the TEM grid after separation from the layer. The SAED patterns were used to calculate the interplanar spacings, which proved the formation of a wurtzite structure ZnO microcrystals (P63 mc, a = 3.2495 Å, c = 0.52069 Å; JCPDS card N 036–1451).

Fig. 2 (d) presents the EDS data on the average composition of the total area depicted in Fig. 2 (b). The direct composition of the microcrystal was obtained by focusing the electron beam on its basal plane and recording its EDS spectrum. The microcrystal consists mainly of Zn and oxygen, with a small addition of carbon and copper (Fig. 2e). The carbon contaminants appear due to exposure of a sample to atmospheric air during its transferring into the SEM chamber. The copper concentration does not exceed 1 at.%. This value is quite below of Cu solubility limit in ZnO (5 at.%. [12]).

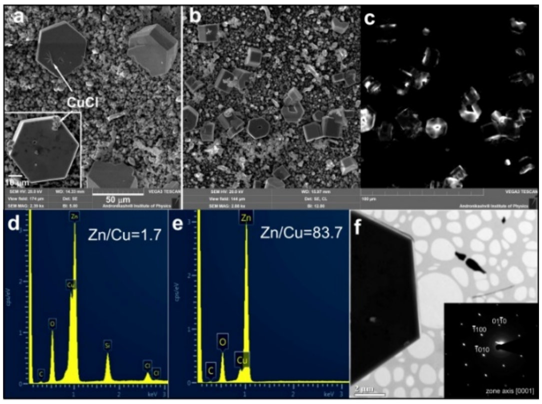

Fig. 2. SEM and cathodoluminescence images of rod-like ZnO crystals grown at 290°C (a,b,c); EDS spectra from the area, depicted in Fig. 2 a, and from the bulk of ZnO microcrystal (d,e); TEM image and SAED pattern of ZnO microcrystal (f).

In the vapor phase we have CuCl, ZnCl and ZnO species. ZnO is formed due to a gas phase reaction of $ZnCl_2(g)$ and oxygen molecules produced after different reactions of CuO and ZnO sources. It was found that the ZnO crystallites were growing only in case if CuO was added to the source and, hence when CuCl was present in the gaseous phase. Below, we will explain the role of CuCl in the growth of ZnO microcrystals.

One of the major subjects of crystal formation is the nucleation and growth mechanisms. As it is shown in Fig. 1, in the first stage of growth the layer of $ZnCl_2$-CuCl was formed on Si at a low substrate temperature. It is established in [6] that the eutectic composition in $ZnCl_2$-CuCl system contains 71 mol.% of $ZnCl_2$, and the melting point drops to 241°C. The sintering of particles and molten droplets were observed in many places of $ZnCl_2$-

CuCl layer grown at 290°C (Fig. 2 a, b). At the local points of a substrate the eutectic compositions of CuCl-$ZnCl_2$ may exist, which will melt as soon as the temperature of $ZnCl_2$-CuCl layer reaches or exceeds 241°C. These molten droplets may serve as effective sinks for ZnO vapor formed in the gaseous phase by the oxidation of $ZnCl_2$ precursors. The oversaturation of a droplet with ZnO will cause the precipitation of a solid ZnO and nucleation of ZnO, the same way as it takes place in the well-established Vapor-Liquid-Solid (VLS) growth of 1D nanomaterials from a molten catalyst tip.

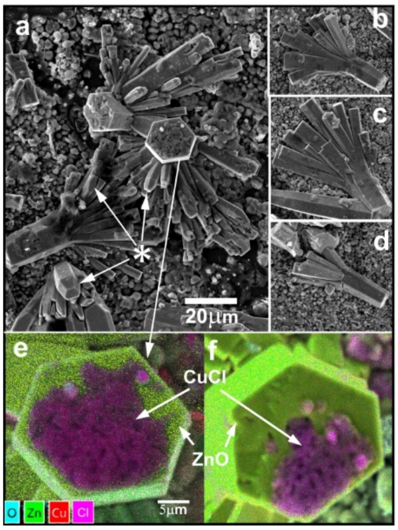

Fig. 3. SEM image of ZnO microcrystals grown at 330°C(a); some examples of multiple nucleation and growth of ZnO on prism planes of the main crystal (b-d); element maps of (0001) plains of the main crystal, covered with CuCl layer (e,f).

As the temperature exceeds the nucleation temperature (~241°C), the CuCl molecules prevail in the vapor. The composition of a layer on Si substrate is enriched with CuCl and the melting point shifts to higher values, causing the solidification of a droplet. After this point, the nucleation stops, and the existing ZnO nuclei are growing-through the slow Vapor-Solid mechanism, producing large ZnO microcrystals. The similar sizes of microcrystals indicate that they were produced simultaneously. The rod-like shape of ZnO proves that the slow growth proceeded at conditions close to equilibrium, causing the lateral and longitudinal growth at a similar rate [13].

Fig. 3 illustrates ZnO microcrystals synthesized at a substrate temperature of 330°C. The sparse crystal growth again takes place. In contrast to crystals grown at 290°C, the intense secondary nucleation on prism planes is observed for microcrystals grown at 330°C. The morphology of ZnO changes from rod-like to elongated, 1D nano-wire-like structures, indicating the increase in the growth rate at elevated temperatures.

The Zn terminated (0001) basal plane of ZnO is the most chemically active one with the highest surface energy (σ=2.0 J/m^2), while the prism planes are characterized by a low energy (σ=1.2 J/m^2 for (10-10) plane) and low activity [5]. Usually, in the fast nonequilibrium crystal growth processes, which include our pyrolytic synthesis technology carried out at 330°C, the growth of wurtzite ZnO proceeds along *c*-axes ([0001] direction). As a result, the elongated hexagonal crystals or hexagonal 1D nanomaterials are formed with a high aspect ratio [14]. Besides, according to classic crystal growth theory, in the fast, non-equilibrium processes, the planes with the highest growth rate tend to vanish with the increase of a growth time, thus causing the gradual decrease of their surface areas and tapering of tips [15]. In our samples, the ZnO growth rate in [0001] direction significantly increased at 330°C. Accordingly, the truncated hexagonal pyramid shaped tapered tips of ZnO were observed, as shown by the arrows in Fig. 3 (a). The (0001) surfaces of newly-formed crystals were free of any contaminants. The surface of the main crystal, formed at 290°C, was barely contaminated with CuCl particles (Fig.2 a, and its inset). However, at elevated temperatures, until the CuO was completely consumed in the source, a part of (0001) surfaces of the main crystals were covered with a layer of CuCl because of the highest chemical activity of a basal plane (Fig. 3 e, f). This layer restricted the growth of secondary ZnO microcrystals on the (0001) plane and remained there even after complete consumption of CuO in the source.

Conclusion

ZnO microcrystals were synthesized at relatively low temperatures (near 300°C)

from $ZnCl_2$ and CuCl vapor. CuCl served to produce the eutectic compositions with $ZnCl_2$, having a low melting point of 241°C. The molten droplets thus formed served as sinks for ZnO molecules synthesized in the gas phase after the interaction of $ZnCl_2$ with oxygen. The oversaturation of droplets with ZnO caused its precipitation and formation of ZnO nuclei, which were then growing through the low-rate thermodynamically driven Vapor-Solid mechanism. As a result, several micrometers-sized rod-like ZnO microcrystals (the main crystals) were formed at a substrate temperature of 290°C. At substrate temperature of 330°C, the intense secondary nucleation on the prism planes of the main crystal was observed, caused by an increase in the ZnO vapor formation. The newly synthesized elongated ZnO crystals with 1D morphology were growing in the [0001] direction, as it is usually observed in fast-growing, kinetically driven ZnO growth processes. No nucleation was seen on the basal (0001) plain of the main crystal, as it was covered with CuCl material, formed at the first stage of the growth.

This work was supported by Shota Rustaveli National Science Foundation of Georgia (SRNSFG) [grant number YS-19-087].

ფიზიკა

თუთიის ოქსიდის მიკროკრისტალების გაზრდა სპილენძისა და თუთიის ქლორიდების წინაპროდუქტებიდან

ა. ჯიშიაშვილი*, ზ. შიოლაშვილი*, დ. ჯიშიაშვილი*, ა. ჭირაქაძე*,
ნ. მახათაძე*

**საქართველოს ტექნიკური უნივერსიტეტი, ვ. ჭავჭანიძის სახელობის კიბერნეტიკის ინსტიტუტი, თბილისი, საქართველო*

(წარმოდგენილია აკადემიის წევრის გ. ჯაფარიძის მიერ)

ნაშრომი ეძღვნება შედარებით დაბალ (~300°C) ტემპერატურაზე $ZnCl_2$ და CuCl-ის ორთქლიდან ZnO-ს მიკროკრისტალების ზრდის მექანიზმის შესწავლას. ნაჩვენებია, რომ 230°C-ზე სილიციუმის ფუძეშრეზე მიიღება თუთიისა და სპილენძის ქლორიდების ფხვიერი ფენა. ორთქლში CuCl-ის არსებობა ემსახურება ფუძეშრის ლოკალურ წერტილებში $ZnCl_2$-თან ევტექტიკური შედგენილობის წარმოქმნას, რომელსაც დაბალი, 241°C-ის ტოლი დნობის ტემპერატურა გააჩნია. როდესაც ფუძეშრის ტემპერატურა აჭარბებს ამ სიდიდეს, ევტექტიკური ნაერთი დნება და ქმნის თხევად წვეთს. თავის მხრივ, წვეთი აქტიურად აბსორბირებს ZnO-ს აირადი ფაზიდან, გადაჯერდება და გამოჰყოფს მყარი ZnO-ს კრისტალურ ჩანასახს.

REFERENCES

1. Galdámez-Martinez A., Santana G., Güell F., Martínez-Alanis P. R., Dutt A. (2020) Photoluminescence of ZnO nanowires: a review. *Nanomaterials.* **10:** 23.
2. Barzinjy A., Hamad S., Azeez H. (2020) Structure, synthesis and applications of ZnO nanoparticles: a review. *Jordan Journal of Applied Science.***13:** 23-135.
3. Shaba E.Y., Jacob J. O., Tijani J.O., Suleiman M.A.T. (2021) A critical review of synthesis parameters affecting the properties of zinc oxide nanoparticle and its application in wastewater treatment. *Applied Water Science*. **11:** 41.
4. Zhang Y., Ram M.K., Stefanakosi E.K. (2012) Synthesis, characterization, and applications of ZnO nanowires. *Journal of Nanomaterials.* **2012:** 22.
5. Saunders R. B., McGlynn E., Henry M. O. (2011) Theoretical analysis of nucleation and growth of ZnO nanostructures. *Crystal Growth & Design.* **11:** 4581–4587.
6. Viitala H., Taskinena P., Lindberg D. (2019) Experimental determination and thermodynamic optimization of the CuCl–$ZnCl_2$ phase equilibria. *Calphad.* **67:** 15.
7. DeMicco G., Fouga G.G., Bohe A.E. (2007) Chlorination of Zinc Oxide between 723 and 973 K. *Metallurgical and Materials Transactions B*. **38B:** 853-862.
8. Magee D.W. (1955) A determination of the vapor pressures of sulfur, mercuric iodide, and cuprous chloride. *Thesis*. The Ohio State University.
9. Acker J., Kother S., Lewis K.M., Bohmhammel K. (2003) The reactivity in the system CuCl-Si related to the activation of silicon. *Silicon Chemistry.* **2:**195–206.
10. Nakamoto K. (2009) Infrared and Raman spectra of inorganic and coordination compounds. John Wiley & Sons, Inc., Hoboken, New Jersey.
11. Jishiashvili D., Chirakadze A., Shiolashvili Z., Makhatadze N., Jishiashvili A. (2019)Vapor synthesis of copper-based nanostructures. *Proceedings of the International Conference Modern Trends in Physics,* 43-46. Baku.
12. Das S., Srivastava V. C. (2018) An overview of the synthesis of CuO-ZnO nanocomposite for environmental applications. *Nanotechnology Reviews.* **7:** 267-282.
13. Ji Sh., Ye Ch. (2008) Synthesis, growth mechanism, and applications of Zinc Oxide ganomaterials. *Journal of Materials Science and Technology.* **24:** 16.
14. Xu Sh., Wang Z. L. (2011) One-dimensional ZnO nanostructures: solution growth and functional properties. *Nano Research*. **4:**1013–1098.
15. Lin L., Fuji M., Watanabe H., Shirai T., Takahashi M. (2008) Potential applications and synthesis of zinc oxide tubes. *Annual Report of Ceramics Fundamental Engineering Research Center,* **8:**17-22, Japan.

Received April, 2021